

# Strong coupling theory of heavy fermion criticality II

## Peter Wölfle

Institute for Theory of Condensed Matter, Karlsruhe Institute of Technology, 76049  
Karlsruhe, Germany

Institute for Nanotechnology, Karlsruhe Institute of Technology, 76031 Karlsruhe,  
Germany

E-mail: peter.woelfle@kit.edu

## Jörg Schmalian

Institute for Theory of Condensed Matter, Karlsruhe Institute of Technology, 76049  
Karlsruhe, Germany

Institute for Solid State Physics, Karlsruhe Institute of Technology, 76031 Karlsruhe,  
Germany

E-mail: joerg.schmalian@kit.edu

## Elihu Abrahams

Department of Physics and Astronomy, University of California Los Angeles, Los  
Angeles, CA 90095

E-mail: abrahams@physics.ucla.edu

10 March 2021

**Abstract.** We present a theory of the scaling behavior of the thermodynamic, transport and dynamical properties of a three-dimensional metal governed by  $d$ -dimensional fluctuations at a quantum critical point, where the electron quasiparticle effective mass diverges. We determine how the critical bosonic order parameter fluctuations are affected by the effective mass divergence. The coupled system of fermions and bosons is found to be governed by two stable fixed points: the conventional weak-coupling fixed point and a new strong-coupling fixed point, provided the boson-boson interaction is irrelevant. The latter fixed point supports hyperscaling, characterized by fractional exponents. The theory is applied to the antiferromagnetic critical point in certain heavy fermion compounds, in which the strong-coupling regime is reached.

## 1. Introduction

The properties of matter at low temperatures has always been a subject of frontier research in theoretical and experimental condensed matter physics. In the case of metallic systems, in particular, this research has led to an appreciation of the crucial

role played by electron-electron interaction effects in determining the character of unexpected new phases that emerge at low temperature. Thus, in recent decades, there have been intensive studies of quantum criticality in metals and magnetic materials. A zero-temperature transition between two distinct ground states, a quantum phase transition, may be realized by tuning some external parameter such as magnetic field, pressure, chemical composition, ... Recent metallic materials realizations of quantum phase transitions include the cuprate superconductors, the iron-based superconductors and the heavy-electron compounds. All these have complex phase diagrams that reflect how strong electron correlation effects determine the character and competition of new phases (*e.g.* magnetism, superconductivity) and behavior that deviates from that of simpler metals, as described by the standard Landau Fermi liquid theory.

Often, a quantum critical point (QCP) marks the transition from a magnetically-ordered phase to a paramagnetic one; associated with it are bosonic quantum fluctuations of the relevant magnetic order parameter. Then, due to the scattering of the fermionic quasiparticles off these fluctuations, there may be significant modifications of Fermi liquid behavior even in the paramagnetic regions of the phase diagram. Quantum phase transitions in itinerant magnetic systems have been theoretically studied using approaches related to that originally proposed by Hertz[1] and further developed by Millis[2] and these have been recently reviewed.[3] The early theories of quantum critical behavior were formulated in the framework of a  $\phi^4$ -field theory defined by a Ginzburg-Landau-Wilson action of an order parameter field  $\phi$ ; they found that since temporal fluctuations increase the effective dimension of the field theory to  $d_{eff} = d + z$  where  $d, z$  are the spatial dimension of the fluctuations and the dynamical critical exponent, it may happen that the theory is essentially Gaussian. This is the case if  $d_{eff} > 4$ , the upper critical dimension, and the fluctuations are effectively non-interacting (for a review see Ref. [3]). The theory for non-metallic systems expressed in terms of a field theory for the order parameter is well-founded; it was developed in Ref. [4]. However, in metallic systems, the fermionic degrees of freedom may become critical themselves and a generalized formulation that treats the critical bosons and fermions on equal footing is called for. The large low-temperature quasiparticle mass enhancements observed in heavy-electron compounds suggest that they are systems in which this situation may occur. It is in this context that a semi-phenomenological theory for quantum criticality was developed [5] and applied[6, 7] to successfully account for experimental observations in the two compounds YbRh<sub>2</sub>Si<sub>2</sub> (YRS) and CeCu<sub>6-x</sub>Au<sub>x</sub> (CCA). In this report, we review the fundamentals of that theory of “critical quasiparticles”, fill in some of the mathematical details and put it on firmer microscopic grounds by deriving the scaling behavior of the thermodynamic, transport and dynamical properties of the metallic quantum critical system.

Contrary to what one might expect, there actually exists a window in parameter space where a consistent theory may be constructed, although the fermionic and bosonic degrees of freedom are strongly coupled. A necessary condition to be fulfilled is, however, that the direct boson-boson coupling is still irrelevant (crudely speaking,  $d_{eff} > 4$ ).

Our theory presents an alternative scenario of quantum criticality in heavy-fermion metals. In these compounds, the accepted scenario is that the Kondo effect leads to the emergence of heavy quasiparticle masses as a consequence of the screening of the localized spins of the rare earth ions by the conduction electrons. This leads to a many-body resonance state at each ion, at which the conduction electrons are resonantly scattered, which slows down their motion through the lattice. On the other hand, the localized spins are coupled by exchange interaction, mediated by the conduction-electron system (RKKY) or by direct exchange. As pointed out early on by Doniach,[8] the competition between exchange and the Kondo effect might lead to an abrupt breakdown of Kondo screening, often called “Kondo breakdown”. Following the experimental discovery of unusual quantum critical behavior in many heavy-fermion compounds, several “Kondo breakdown” scenarios have been proposed.[9] One of these involves a local transition of the Kondo resonance state at the antiferromagnetic transition, giving rise to “local quantum criticality”. A somewhat similar proposal invokes an “orbitally selective Mott transition” involving the abrupt vanishing of the hybridization of  $f$  electrons and conduction electrons within an Anderson lattice model, and hence a sharp transition between the itinerant heavy-fermion state and a localized  $f$ -electron spin state. This picture has been realized using slave-boson mean field theory [10] and cellular-DMFT calculations.[11] Yet another scenario proposes a fractionalization of the heavy quasiparticles into spin and charge carrying components driven by strong frustration and/or quantum fluctuations,[12] leading to the formation of a spin liquid state [13, 14] dubbed “fractionalized Fermi liquid” or FL\*. The latter may undergo a transition into a usual antiferromagnetic phase. A third possibility is given by a Fermi surface reconstruction inside the antiferromagnetically ordered phase, as the hybridization of  $f$ -electrons and conduction electrons is tuned through a critical value, changing the large Fermi surface of the heavy quasiparticles into the small Fermi surface of light conduction electrons. The latter has apparently been observed in some of the CeMIn<sub>5</sub> compounds (M stands for a transition metal ion).[15, 16, 17] It has also been recognized that the two phases, heavy quasiparticles in the paramagnetic phase and localized ordered spins weakly coupled to conduction electrons may be adiabatically connected.[18] An adiabatic connection of states characterized by large and small Fermi surfaces is indeed possible in the antiferromagnetic phase, where the Fermi surfaces are downfolded into the magnetic Brillouin zone and the meaning of large and small Fermi surface may be lost. We assume here that the latter scenario is applicable, *i.e.* one has a smooth crossover from large heavy-fermion Fermi surface to ordered local moments, as one moves deeper into the antiferromagnetic phase. This assumption appears justified in the case of the two heavy fermion compounds on which we focus, CeCu<sub>6-x</sub>Au<sub>x</sub> at  $x \approx 0.1$  and YbRh<sub>2</sub>Si<sub>2</sub>. For the latter, YRS, various anomalies were observed along a  $T^*$ -line in the temperature-magnetic field phase diagram.[19] These were initially interpreted as a consequence of “Kondo breakdown.” However, ARPES studies [20] do not give an indication for a Fermi surface reconstruction. Recently, the anomalies observed along the  $T^*$ -line have been shown to arise from a freezing out of spin-flip scattering.[21]

## 2. Critical Fermi liquid

The unusual properties of metals observed near quantum critical points have often been termed “non-Fermi liquid behavior”. Rather than describing such a state as what it is not, we shall call it a “critical Fermi liquid” and its low-lying excitations “critical quasiparticles”. While it is true that at zero temperature  $T = 0$  and zero excitation energy  $\omega = 0$  fermionic quasiparticles may no longer exist, we shall demonstrate that at any non-zero  $T, \omega$ , fermionic quasiparticles are still well-defined for a class of critical states. As first introduced by Landau, fermionic quasiparticles are defined by the poles of the single particle Green’s function  $G(\mathbf{k}, \omega)$  in the complex frequency plane. The retarded Green’s function is given in terms of the self energy  $\Sigma(\mathbf{k}, \omega)$  as

$$G_\sigma(\mathbf{k}, \omega + i0) = \frac{1}{\omega - \epsilon_{\mathbf{k}} - \Sigma_\sigma(\mathbf{k}, \omega + i0)} \quad (1)$$

where  $\sigma$  is the spin quantum number. For the moment, we assume that the dependence of  $\Sigma$  on  $\mathbf{k}$  is weak and may be neglected. We shall return to this issue later. When the Green’s function has a (quasiparticle) pole at  $\omega = \epsilon_{\mathbf{k}}^*$ , we may expand  $\Sigma$  near it as  $\Sigma_\sigma(\mathbf{k}, \omega + i0) = \text{Re}\Sigma_\sigma(\mathbf{k}, \epsilon_{\mathbf{k}\sigma}^*) + i\text{Im}\Sigma_\sigma(\mathbf{k}, \epsilon_{\mathbf{k}\sigma}^*) + (\omega - \epsilon_{\mathbf{k}\sigma}^*)\partial\text{Re}\Sigma_\sigma(\mathbf{k}, \omega)/\partial\omega|_{\omega=\epsilon_{\mathbf{k}\sigma}^*} + \dots$  such that the Green’s function may be expressed in terms of a quasiparticle term and an incoherent background contribution:  $G_\sigma = G_\sigma^{qp} + G_\sigma^{inc}$ , where

$$G_\sigma^{qp}(\mathbf{k}, \omega + i0) = \frac{Z_\sigma(\mathbf{k}, \epsilon_{\mathbf{k}\sigma}^*)}{\omega - \epsilon_{\mathbf{k}\sigma}^* + i\Gamma_\sigma(\mathbf{k}, \epsilon_{\mathbf{k}\sigma}^*)} \quad (2)$$

with  $[Z_\sigma(\mathbf{k}, \epsilon_{\mathbf{k}\sigma}^*)]^{-1} = 1 - \partial\text{Re}\Sigma_\sigma(\mathbf{k}, \omega)/\partial\omega|_{\omega=\epsilon_{\mathbf{k}\sigma}^*}$  and  $\Gamma_\sigma(\mathbf{k}, \epsilon_{\mathbf{k}\sigma}^*) = Z_\sigma(\mathbf{k}, \epsilon_{\mathbf{k}\sigma}^*)\text{Im}\Sigma_\sigma(\mathbf{k}, \epsilon_{\mathbf{k}\sigma}^*)$ . The quasiparticle contribution to the spectral function  $\mathcal{A}^{qp} = (-1/\pi)\text{Im}G^{qp}$  is then

$$\mathcal{A}_\sigma^{qp}(\mathbf{k}, \omega) = \frac{Z_\sigma(\mathbf{k}, \epsilon_{\mathbf{k}}^*)\Gamma_\sigma(\mathbf{k}, \epsilon_{\mathbf{k}}^*)/\pi}{[\omega - \epsilon_{\mathbf{k}}^*]^2 + \Gamma_\sigma(\mathbf{k}, \epsilon_{\mathbf{k}}^*)^2} \quad (3)$$

It is seen that  $\mathcal{A}(\omega)$  has a quasiparticle peak at  $\omega = \epsilon_{\mathbf{k}}^*$ , provided  $\Gamma < \epsilon_{\mathbf{k}}^*$ . In that case,  $\mathcal{A}(\omega) \approx Z(\omega)\delta(\omega - \epsilon_{\mathbf{k}}^*)$ , we may replace  $\epsilon_{\mathbf{k}}^*$  by  $\omega$  and observe that  $\epsilon_{\mathbf{k}}^* \approx Z\epsilon_{\mathbf{k}}$  so that we may interpret  $1/Z$  as a correlation-induced mass enhancement  $m^*/m$ . We now explore the possibility of using the notion of fermionic quasiparticles even when the quasiparticle weight  $Z_\sigma(\mathbf{k}, \omega) \rightarrow 0$  as  $\omega \rightarrow 0$ . As long as  $\omega \neq 0$  (or else  $\omega = 0$ , but  $T \neq 0$ ), so that  $Z \neq 0$ , what we defined as the quasiparticle contribution to  $G$  does exist. The question is whether it is well-defined. We have seen that a quasiparticle peak in the spectral function exists if the decay rate  $\Gamma(\omega)$  (the width of the peak) is less than the energy at the peak position, Consider the situation of a self energy that varies with frequency as

$$\Sigma(\omega) \propto i(i\omega)^{1-\eta} = i(\cos\phi + i\sin\phi)|\omega|^{1-\eta}, \quad 0 < 1 - \eta < 1, \quad (4)$$

where  $\phi = \text{sign}(\omega)(1 - \eta)\pi/2$ . We shall see that this behavior is actually found near a QCP. This form is chosen such that  $\text{Im}\Sigma > 0$ , but  $\text{Re}\Sigma \propto \text{sign}(\omega)$ , as required by Fermi statistics and the analyticity properties of  $\Sigma$ . We note that  $\text{Re}\Sigma \propto \text{Im}\Sigma \propto |\omega|^{1-\eta}$ . Here we have suppressed the momentum dependence of  $\Sigma$  for simplicity. It follows that at low frequency,  $Z(\omega) \propto |\sin\phi|^{-1}(1 - \eta)^{-1}|\omega|^\eta$ , so that the quasiparticle decay rate  $\Gamma(\omega) = Z(\omega)\text{Im}\Sigma(\omega) \propto (1 - \eta)^{-1} \cot[(1 - \eta)\pi/2]|\omega|$  is a linear function of  $\omega$  independent

of  $\eta$ . From these considerations, we may deduce the condition on the exponent  $\eta$  such that coherent quasiparticles exist, *i.e.*  $\Gamma(\omega) < \omega$ . We see that it is required that

$$\cot[(1 - \eta)\pi/2] < (1 - \eta) \rightarrow \eta < 0.36. \quad (5)$$

We shall see that this condition has important consequences when the self energy varies around the Fermi surface.

When  $Z \propto |\omega|^\eta$ , the quasiparticle effective mass will be scale-dependent,  $m^* = m^*(\omega) \propto Z^{-1} \propto |\omega|^{-\eta}$ . The effective mass is a measure of the scale dependent quasiparticle density of states  $N^*(\omega) \propto m^*(\omega)$ , which enters the specific heat coefficient  $\gamma(T) = C(T)/T \propto N^*(T)$ . So whenever the experimentally determined  $\gamma(T)$  appears to diverge in the neighborhood of a QCP, we may assume the fermionic quasiparticles to be critical.

Whether or not the momentum dependence of the self energy may be neglected, as assumed above, depends on the microscopic processes that contribute to it. As mentioned in Sec. I, this is often the scattering of the quasiparticles off quantum critical fluctuations of the order parameter. In the case of incommensurate antiferromagnetic or charge density wave order, these fluctuations are at some wavevector(s)  $\mathbf{Q}$  that connect discrete sets of points on the Fermi surface, the so-called ‘‘hot spots’’. For quasiparticles near the hot spots, the momentum dependence of  $\Sigma$  may not be neglected. We will take this dependence into account in the following.

### 3. Renormalized perturbation theory of self energy and vertex function.

The critical spin fluctuations near a quantum critical point separating paramagnetic and antiferromagnetic phases are described by the dynamical spin susceptibility  $\chi(\mathbf{q}, \nu)$  at wave vectors  $\mathbf{q}$  near the ordering wave vector  $\mathbf{Q}$ . We assume incommensurate antiferromagnetic order, *i.e.*  $\mathbf{Q}$  is not a reciprocal lattice vector, as is most often the case in metallic antiferromagnets. The generic form of  $\chi(\mathbf{q}, \nu)$  is

$$\chi(\mathbf{q}, \nu) = \frac{N_0}{r + (\mathbf{q} - \mathbf{Q})^2 \xi_0^2 - i\Lambda_Q^2(\nu/v_F Q)} \quad (6)$$

where  $N_0$  is the bare density of states at the Fermi level,  $r$  is the control parameter tuning the system through the QCP,  $\xi_0 \approx k_F^{-1}$  is a microscopic correlation length,  $v_F = k_F/m$  is the bare Fermi velocity, and  $\Lambda_Q = \Lambda(\mathbf{k}, \omega = 0; \mathbf{q}, \nu)$  is the vertex function at the antiferromagnetic spin fluctuation-particle-hole vertex, *i.e.* the vertex at non-zero momentum  $\mathbf{q} \approx \mathbf{Q}$ . The physical (renormalized) susceptibility is determined by the structure and dynamics of the underlying electron degrees of freedom. This is reflected in Eq. (6) by the appearance of  $\Lambda_Q$  in the Landau damping term in the denominator. It may be shown that when  $Z^{-1}(\omega) \propto m^*(\omega)/m$  diverges, then the vertex  $\Lambda_Q \sim Z^{-1}$  will diverge as well (Ref. [22] and below). The dynamical properties (self energy, vertex function) of the critical Fermi liquid will be determined by the scattering of the quasiparticles from the renormalized critical fluctuations. It follows that  $\chi(\mathbf{q}, \nu)$  depends on the critically enhanced effective mass. Likewise, the effective mass enhancement following

from scattering of quasiparticles off spin fluctuations depends on the spectral density of spin fluctuations. The resulting set of self-consistent equations for the effective mass and the vertex function supports new strong coupling solutions as will be shown below.

As will be reviewed in the next subsection, the self energy and the vertex functions are strongly dependent on the position on the Fermi surface. In particular, for scattering by a single spin fluctuation, involving the large momentum transfer  $\mathbf{Q}$ , the hot spots consist of a limited manifold of  $\mathbf{k}$ -states on the Fermi surface. This manifold comprises those wavevectors  $\mathbf{k}_h$  that satisfy the condition that  $\mathbf{k}_h$  and  $\mathbf{k}_h \pm \mathbf{Q}$  are both near the Fermi surface. Landau damping involves the decay of spin fluctuations of frequency  $\nu$  and momentum  $\mathbf{q}$  into particle-hole pairs of momenta  $\mathbf{k} + \mathbf{q}$  and  $\mathbf{k}$  close to the Fermi surface, within an energy range of order  $\max\{\nu, T\}$ . At momenta  $\mathbf{q}$  sufficiently close to the ordering momentum  $\mathbf{Q}$  these particle-hole pairs will be in the hot spots. Below we will estimate the extension of the hot spots on the Fermi surface as  $|\delta\mathbf{k}_h| \approx k_F |\nu/\epsilon_F|^{1/2} \Lambda_Q$ . When  $\mathbf{q}$  deviates from  $\mathbf{Q}$  by more than  $|\delta\mathbf{k}_h|$ , the particle hole pairs involved in the Landau damping will be outside the hot spots. In the calculation of the self energy, which follows in the next section, it will be seen that the wavevectors of the relevant fluctuations contributing to the self energy satisfy exactly this condition, namely  $|\mathbf{q} - \mathbf{Q}| \gg \delta k_h \sim \nu^{1/2} \Lambda_Q$ . We therefore conclude that the vertex function  $\Lambda_Q$  appearing in the Landau damping is actually the one for the cold quasiparticles.

### 3.1. Self Energy $\Sigma$

*3.1.1. One-loop approximation* In one-loop approximation, *i.e.* scattering from a single spin fluctuation, the imaginary part of the self-energy for a “hot” quasiparticle is given by

$$\begin{aligned} \text{Im}\Sigma^{(a)}(\mathbf{k}, \omega) &= u^2 \Lambda_{Q,h}^2 \int \frac{d\nu}{2\pi} \int \frac{d^d q}{(2\pi)^d} \text{Im}G(\mathbf{k} + \mathbf{q}, \omega + \nu) \\ &\quad \times \text{Im}\chi(\mathbf{q}, \nu)[b(\nu) + f(\omega + \nu)], \end{aligned} \quad (7)$$

where  $b(\nu) = 1/(e^{\nu/T} - 1)$  and  $f(\omega) = 1/(e^{\omega/T} + 1)$  are the Bose and Fermi functions,  $u \approx N_0^{-1}$  is the boson-fermion interaction and  $\Lambda_{Q,h}$  is the relevant vertex function (see above). In the limit of low excitation energy,  $\omega \rightarrow 0$  and at the Fermi surface,  $\epsilon_{\mathbf{k}} = 0$ , we take into account that the main contribution to the integrals is from small  $\nu$ , so we may approximate  $\text{Im}G$  by its quasiparticle component,  $\text{Im}G^{qp}(\mathbf{q} + \mathbf{k}, \nu + \omega) \approx \pi Z \delta(\omega + \nu - \epsilon_{\mathbf{k}+\mathbf{q}}^*)$ , as already mentioned below Eq. (3). We now shift the momentum vector  $\mathbf{q} \rightarrow \mathbf{q} + \mathbf{Q}$ , such that the peak of  $\chi$  shifts to  $\mathbf{q} = 0$  and  $\epsilon_{\mathbf{k}+\mathbf{q}}^* \rightarrow \epsilon_{\mathbf{k}+\mathbf{q}+\mathbf{Q}}^*$ . We expand the quasiparticle energy  $\epsilon^*$  in both small  $q$  and small deviation  $\delta\mathbf{k}$  from the hot spot momentum, so that  $\epsilon_{\mathbf{k}_h+\mathbf{Q}+\mathbf{q}+\delta\mathbf{k}}^* \approx q|v_{\mathbf{k}_h+\mathbf{Q}}^*| \cos\theta + \delta\epsilon_{\mathbf{k}}^*$ , where  $\delta\epsilon_{\mathbf{k}}^* = \delta\mathbf{k} \cdot \mathbf{v}_{\mathbf{k}_h+\mathbf{Q}}^* + O(\delta\mathbf{k}^2)$  and  $\theta$  is the angle subtended by the vectors  $\mathbf{q}$  and  $\delta\mathbf{k}$ . We have set  $\epsilon_{\mathbf{k}_h+\mathbf{Q}}^* = 0$ , since  $\mathbf{k}_h + \mathbf{Q}$  is on the Fermi surface. We perform the angular integral:

$$\int d\Omega_q \text{Im}G^{qp}(\mathbf{k}_h + \mathbf{q}, \omega + \nu) \propto \frac{1}{v_F q} \Theta(qv_F^* - |\delta\epsilon_{\mathbf{k}}^*|), \quad (8)$$

where  $\Theta(x)$  is the unit step function. In the limit of low  $T \ll \omega$  the  $\nu$ -integral extends over the interval  $[0, \omega]$ . The  $q$ -integral is governed by the lower limit  $q_l \approx [(|\nu|\Lambda_Q^2)^2 + (\delta\mathbf{k})^4]^{1/4}$ , as determined by the theta function of Eq. (8) and the denominator of  $\text{Im}\chi(\mathbf{q}, \nu)$  from Eq. (6), where we set  $v_F Q \approx \epsilon_F$  (as  $Q$  is usually of order  $k_F$ ). Here and in what follows we have set  $\xi_0 \approx 1/k_F$  and used  $k_F, \epsilon_F$  as units for wave vectors and energies or frequencies. Then

$$\begin{aligned} \text{Im}\Sigma^{(a)}(\mathbf{k}, \omega) &\propto u^2 \Lambda_{Q,h}^2 N_0 \xi_0^{-4} v_F^{-1} \int_0^\omega d\nu \frac{\nu}{\epsilon_F} \Lambda_Q^2 \int_{q_l} \frac{dq}{q^{6-d}} \\ &\propto \Lambda_{Q,h}^2 \Lambda_Q^{d-3} \epsilon_F \{[\omega^2 + x_{\mathbf{k}}^2]^{(d-1)/4} - x_{\mathbf{k}}^{(d-1)/2}\}, \end{aligned} \quad (9)$$

where  $x_{\mathbf{k}} = (\delta\mathbf{k}/\Lambda_Q)^2$ . Therefore

$$\text{Im}\Sigma^{(a)}(\mathbf{k}, \omega) \propto \begin{cases} \Lambda_{Q,h}^2 \Lambda_Q^{d-3} |\omega|^{(d-1)/2}, & |\omega| > x_{\mathbf{k}} \\ \Lambda_{Q,h}^2 \Lambda_Q^2 \omega^2 / (\delta\mathbf{k})^{5-d}, & |\omega| < x_{\mathbf{k}}. \end{cases} \quad (10)$$

The extension of the hot spots in momentum space for given energy  $\omega$  can be read off (after reinstalling conventional units) as  $(\delta k_\perp/k_F) \approx (\omega/\epsilon_F)^{1/2} \Lambda_Q \cos \alpha$  and  $(\delta k_\parallel/k_F) \approx (\omega/\epsilon_F)^{1/2} \Lambda_Q \sin \alpha$  for deviations  $\delta\mathbf{k}$  normal and parallel to the Fermi surface, respectively. Here  $\alpha$  is the angle subtended by  $\mathbf{v}_{\mathbf{k}_h}$  and  $\mathbf{v}_{\mathbf{k}_h+\mathbf{Q}}$ , which is expected to be of order  $\pi/2$ . We denoted the vertex functions at the hot spots by  $\Lambda_{Q,h}$ , while  $\Lambda_Q$  refers to the cold part of the Fermi surface.

From these results, we can find the real part of  $\Sigma$  by Kramers-Kronig transform and finally the quasiparticle  $Z$ -factor as follows:

$$\text{Re}\Sigma^{(a)}(\mathbf{k}, \omega) = \left( \int_{x_{\mathbf{k}}}^{\omega_0} + \int_0^{x_{\mathbf{k}}} \right) d\omega' \frac{\omega \text{Im}\Sigma^{(a)}(\mathbf{k}, \omega')}{\omega'^2 - \omega^2} = \Sigma_h + \Sigma_l \quad (11)$$

Carrying out the calculation for a wavevector  $\mathbf{k}$  on a cold part of the Fermi surface, one finds that the self energy  $\Sigma^{(a)}(\mathbf{k}, \omega)$  has no singular behavior in  $\omega$ . This may already be seen from the above expression for  $\text{Im}\Sigma$ . Of course, it is expected that singular behavior due to single spin fluctuation scattering will only occur at the hot spots. Therefore, we may now take  $x_{\mathbf{k}} = (\delta\mathbf{k}/\Lambda_Q)^2 \approx 0$  and find.

$$\begin{aligned} \Sigma_h &\approx -\omega \Lambda_{Q,h}^2 \Lambda_Q^{d-3} \left( \int_0^{\omega_0} d\omega' \frac{\omega'^{(d-1)/2}}{\omega'^2 - \omega^2} \approx \int_\omega^{\omega_0} \omega'^{(d-5)/2} d\omega' \right) \\ &= -\omega \Lambda_{Q,h}^2 \Lambda_Q^{d-3} |\omega|^{(d-3)/2} \end{aligned} \quad (12)$$

$$\Sigma_l \approx 0 \quad (13)$$

The contribution to the quasiparticle weight factor from spin fluctuations is obtained as

$$\begin{aligned} Z_S^{-1}(\mathbf{k}_h, \omega) &= 1 - \frac{\partial \text{Re}\Sigma^{(a)}(\mathbf{k}_h, \omega)}{\partial \omega} \\ &= \begin{cases} 1 - c_{Z,3} \Lambda_{Q,h}^2 \ln |\omega|, & d = 3 \\ 1 + c_{Z,2} \Lambda_{Q,h}^2 \Lambda_Q^{-1} |\omega|^{-1/2}, & d = 2. \end{cases} \end{aligned} \quad (14)$$

Here, the  $c_{Zs}$  are constants of order unity. To be precise, the vertex  $\Lambda_{Q,h}$  in this analysis connects a hot spot  $\mathbf{k}_h$  to  $\mathbf{k}_h + \mathbf{Q} + \mathbf{q}$  on the cold part of the Fermi surface. This will be taken into account below.

Inspection of Eq. (9) shows that the momentum dependence of  $\Sigma^{(a)}(\mathbf{k}, \omega)$  also becomes critical. However, it will be shown later (Sec. IV) that altogether, the critical renormalizations are so strong in the hot regions that a quasiparticle description is no longer valid there.

So far, we have assumed that the spatial dimension of fermions and bosons is the same. However, it frequently happens that the wavevector of the spin fluctuations is quasi-two-dimensional, *e.g.* located in the  $xy$  plane, while the Fermi surface is that of a three-dimensional system. In this case the manifold of hot momenta is a non-zero fraction of the Fermi surface. For momenta  $\mathbf{k}$  in the manifold of hot momenta, in addition to the integrations above for  $d = 2$ , there is the integral over the component  $q_z$  along the third dimension:

$$\int dq_z \text{Im}G(\mathbf{k}_h + \mathbf{q}, \omega + \nu) \propto \frac{1}{v_F} \quad (15)$$

It follows that

$$\begin{aligned} \text{Im}\Sigma^{(a)}(\mathbf{k}_h, \omega) &\propto u^2 \Lambda_Q^2 N_0 \xi_0^{-4} v_F^{-1} \int_0^\omega d\nu \frac{\nu}{\epsilon_F} \Lambda_Q^2 \int_{q_i} \frac{dq}{q^3} \\ &\propto \Lambda_{Q,h}^2 |\omega| \end{aligned} \quad (16)$$

which is identical with the above result, Eq. (14) at  $d = 3$ .

*3.1.2. Two-loop approximation* A contribution to the electron self energy that is critical everywhere on the Fermi surface is generated by the exchange of *two* spin fluctuations, with nearly vanishing total momentum. Consider an exchange energy density determined by  $J\vec{S}_i \cdot \vec{S}_j$ . Its correlator has the form  $K_E \sim \langle (\vec{S}_i \cdot \vec{S}_j)(\vec{S}_k \cdot \vec{S}_l) \rangle$ , which contains two spin fluctuation propagators in its “disconnected part”:

$$K_E \sim \langle S_i^+ S_l^- \rangle \langle S_k^+ S_j^- \rangle.$$

This motivates our definition of an “energy fluctuation” propagator  $\chi_E$ , built from two spin fluctuations, see Fig. 1 as

$$\begin{aligned} \text{Im}\chi_E(k, k'; \mathbf{q}, \nu) &= \sum_{\mathbf{q}_1, \nu_1} G_{k+\mathbf{q}_1} G_{k'+\mathbf{q}_1-\mathbf{q}} \text{Im}\chi(\mathbf{q}_1, \nu_1) \\ &\quad \times \text{Im}\chi(\mathbf{q}_1 - \mathbf{q}, \nu_1 - \nu) [b(\nu_1 - \nu) - b(\nu_1)], \end{aligned} \quad (17)$$

where  $b(\nu)$  is the Bose function and  $k, k', q$  denote “four-momenta”, *e.g.*  $(\mathbf{k}, \omega)$ . Assuming the external four momenta  $k, k'$  to be “on-shell”, *i.e.* ( $k \approx k_F, \omega \approx 0$ ) and  $q$  small, the Green’s functions  $G_{k+\mathbf{q}_1}, G_{k'+\mathbf{q}_1-\mathbf{q}}$  are off-shell for most values of the momenta  $\mathbf{k}, \mathbf{k}', \mathbf{q}_1$  (the cold part of the Fermi surface) and each may be replaced by  $1/\epsilon_F$ ; this removes the dependence on  $k, k'$  from  $\chi_E$ . There are actually two relevant diagrams here as shown in Fig. 1: diagram (A) with parallel and diagram (B) with crossed  $\chi$ -lines. In the approximation of replacing the intermediate  $G$ ’s by  $1/\epsilon_F$ , the two diagrams have identical momentum and frequency dependence, but differ in spin dependence. Denoting the spins of the incoming and outgoing particle-hole pairs by  $(\alpha, \beta)$  and  $(\alpha', \beta')$  one finds  $\chi_{E;\alpha\beta,\alpha'\beta'}^{A,B}(k, k'; \mathbf{q}, \nu) \propto \mp [3\delta_{\alpha\beta}\delta_{\alpha'\beta'} \pm 2\sigma_{\alpha\beta} \cdot \sigma_{\beta'\alpha'}]$  Here the overall sign is different owing



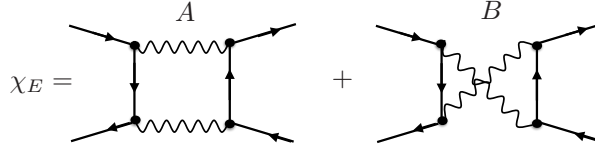


**Figure 1.** Structure of the energy fluctuation. The spin fluctuations  $\chi$  (wavy lines) carry momentum  $\approx Q$ .

to an additional fermion loop in diagram A. The sum of the two contributions gives a pure spin-spin dependence  $\chi_{E;\alpha\beta,\alpha'\beta'} \propto \sigma_{\alpha\beta} \cdot \sigma_{\beta'\alpha'}$ .

Performing the momentum integration in Eq. (17) by Fourier transform, one finds

$$\text{Im}\chi_E(\mathbf{q}, \nu) \approx N_0^3 \Lambda_Q^{2d-3} \left(\frac{|\nu|}{\epsilon_F}\right)^{d-1/2} \frac{1}{\left[r + q^2 \xi_0^2 + |\nu| \Lambda_Q^2 / \epsilon_F\right]^{(d+1)/2}}, \quad (18)$$

One factor of  $N_0$  comes from the momentum integration, the other two from the two spin fluctuation propagators.

The energy-fluctuation propagator  $\chi_E$  may be considered as an exchange boson that generates an effective interaction  $V_E(\mathbf{q}, \nu)$  between quasiparticles. Since  $\chi_E$  couples to a particle-hole (“p-h”) pair,  $V_E$  is screened by p-h polarization effects, represented by the polarization function  $\Pi(\mathbf{q}, \nu)$ , so that

$$V_E(\mathbf{q}, \nu) = \frac{u_E^2 [\Lambda_E \cdot \chi_E(\mathbf{q}, \nu)]}{1 + u_E^2 \Pi(\mathbf{q}, \nu) [\Lambda_E \cdot \chi_E(\mathbf{q}, \nu)]} \quad (19)$$

Here  $\Lambda_E = \Lambda_v^2 \Lambda_Q^4$  is an overall vertex factor arising from vertex functions of two types: first, there arises a vertex function  $\Lambda_Q$  at each end of a spin fluctuation propagator, on the cold part of the Fermi surface. As already mentioned, it diverges as  $Z^{-1}$  (Ref. [22] and below), second, at the ends of the composite propagator  $\chi_E$  a vertex function  $\Lambda_v$  arises. Both vertex corrections are generated only by irreducible diagrams (the reducible parts are either incorporated in  $\chi$ , or explicitly summed, as expressed in Eq. (19)). The Ward identity based on particle number conservation, gives  $\lim_{\nu \rightarrow 0} \Lambda_v(\mathbf{q} = 0, \nu) \propto Z^{-1}$ , but see the discussion below Eq. (36). Finally,  $u_E \propto u^2 \propto N_0^{-2}$  is the bare interaction vertex connecting a p-h pair and an energy fluctuation. We shall see below that  $[\Lambda_E \cdot \chi_E(\mathbf{q}, \nu)]$  also diverges in the limit  $\mathbf{q} = 0, \nu \rightarrow 0$  as  $Z^{-1}$ . This might lead to the expectation that the screening expressed in Eq. (19) will remove the singular behavior of  $V_E$ . This is not the case, since in the denominator of Eq. (19) the divergence of  $[\Lambda_E \cdot \chi_E]$  is removed by the vanishing of the quasiparticle polarization bubble  $\Pi \propto Z$ . As introduced here,  $\Pi$  is the bubble diagram without vertex corrections, as those are included in  $\Lambda_E$ . The screening

thus amounts to a renormalization of  $V_E$  by a factor of order unity, which we neglect in the following, where we analyze quasiparticle scattering off energy fluctuations  $\chi_E$ . We note in passing that the effective interaction of Eq. (19) gives rise to quantum corrections to the conductivity of disordered metals near an antiferromagnetic transition.[23]

In one-loop approximation in terms of the quasi-boson propagator  $\chi_E$ , the imaginary part of the self energy in the cold regions is given by

$$\begin{aligned} \text{Im}\Sigma_c^{(b)}(\mathbf{k}, \omega) &\propto u_E^2 \Lambda_v^2 \Lambda_Q^4 \int \frac{d\nu}{2\pi} \int \frac{d^d q}{(2\pi)^d} \text{Im}G(\mathbf{k} + \mathbf{q}, \omega + \nu) \\ &\quad \times \text{Im}\chi_E(\mathbf{q}, \nu)[b(\nu) + f(\omega + \nu)]. \end{aligned} \quad (20)$$

As in the evaluation of the one-loop self energy contribution of spin fluctuations, Eq. (7), the  $\nu$ -integration at low  $T$  is confined to the interval  $[0, \omega]$  and  $\text{Im}G(\mathbf{k} + \mathbf{q}, \omega + \nu) = \pi Z \delta(\omega + \nu - \epsilon_{\mathbf{k}}^* - v_{\mathbf{k}q}^* \cos \theta)$ , where  $\theta$  is the angle enclosed by  $(\mathbf{k}, \mathbf{q})$ . The angular integral is

$$\int d \cos \theta \text{Im}G(\mathbf{k} + \mathbf{q}, \omega + \nu) \propto \frac{Z}{v_{\mathbf{k}q}^*} \propto \frac{1}{v_F q}. \quad (21)$$

$\text{Im}\chi_E$  is given in Eq. (18). The  $q$ -integration may be done approximately by recognizing that the integral is again controlled by the lower cutoff  $q_l = \xi_0^{-1}(\nu \Lambda_Q^2 / \epsilon_F)^{1/2}$ , now determined by the denominator of Eq. (18):

$$\begin{aligned} \text{Im}\Sigma_c^{(b)}(\mathbf{k}, \omega) &\propto u_E^2 N_0^3 \Lambda_v^2 \Lambda_Q^{2d+1} \int_0^\omega d\nu \nu^{d-1/2} q_l^{-2}(\nu) \\ &\approx \Lambda_v^2 \Lambda_Q^{2d-1} |\omega|^{d-1/2}. \end{aligned} \quad (22)$$

The real part of  $\Sigma$  follows by analyticity as

$$\text{Re}\Sigma^{(b)}(\mathbf{k}, \omega) \propto -\text{sign}(\omega) \Lambda_v^2 \Lambda_Q^{2d-1} |\omega|^{d-1/2} \quad (23)$$

and the contribution of energy fluctuations to the  $Z$ -factor at cold regions is thus obtained as

$$Z_c^{-1} = 1 + b_Z \Lambda_v^2 \Lambda_Q^{2d-1} |\omega|^{d-3/2}, \quad (24)$$

where  $b_Z$  is a constant of order unity. We recall that the exchange of a single spin fluctuation does not lead to a scaling contribution to  $Z^{-1}$  on the cold parts of the Fermi surface. If  $\mathbf{k}$  were to be at a hot region of the Fermi surface, these results still apply, with  $Z_c$  replaced by  $Z_h$ . In the following,  $Z_c$  is usually replaced by simply  $Z$ , as the cold regions are the majority of the Fermi surface.

Higher order contributions are likely to be irrelevant. In Appendix A we show that two-loop contributions to the self energy in energy fluctuation language (four-loop in the spin fluctuation framework) are smaller than the one-loop result  $\propto \omega^{1-\eta}$  by a factor  $\omega^{1-3\eta} \rightarrow 0$  as  $\omega \rightarrow 0$  for dimensions  $3/2 < d < 9/2$ . We introduced the exponent  $\eta$  in Sec. II for the frequency dependence of the  $Z$ -factor. It will be determined self-consistently as  $\eta = (2d - 3)/4d$  in Sec. IV.

3.1.3. *Total self energy* We now collect the results for the self energy. On the cold parts of the Fermi surface we only have a contribution from the scattering off energy fluctuations

$$Z_c^{-1} = 1 + Y_c \quad (25)$$

$$Y_c = b_Z \Lambda_v^2 \Lambda_Q^{2d-1} |\omega|^{d-3/2}, \quad (26)$$

whereas at the hot parts both energy and spin fluctuation scatterings contribute

$$Z_h^{-1} = 1 + Y_h + X_h \quad (27)$$

$$Y_h = b_Z \Lambda_{v,h}^2 \Lambda_Q^{2d-1} |\omega|^{d-3/2} \quad (28)$$

$$X_h = c_Z \Lambda_{Q,h}^2 \Lambda_Q^{d-3} |\omega|^{(d-3)/2} \quad (29)$$

In the latter, we keep in mind that  $\lim_{\epsilon \rightarrow 0} |\omega|^\epsilon \rightarrow \ln(1/|\omega|)$ .

### 3.2. Vertex function $\Lambda_Q$

To complete the self-consistent program for the determination of the  $Z$  factors, we need expressions for the vertex functions. The vertex  $\Lambda_Q$  is obtained as the sum of all p-h-irreducible three-point diagrams at non-zero momentum  $\Lambda_Q(\mathbf{k}, \omega; \mathbf{q}, \nu)$ ,  $\mathbf{q} \approx \mathbf{Q}$ , connecting a particle-hole pair with momenta  $(\mathbf{k} + \mathbf{q}, \omega + \nu)$  and  $(\mathbf{k}, \omega)$  to a spin density fluctuation of momentum  $(\mathbf{q}, \nu)$ . See Fig. 2. It is important to realize that the vertex correction involves only p-h-irreducible diagrams. The reducible diagrams are already incorporated in the spin fluctuation propagator. As shown in Appendix B, the vertex corrections on the cold part of the Fermi surface arising from single spin fluctuation or energy fluctuation exchange are small, in that they invariably include the small factor  $|\omega|/\epsilon_F$ .

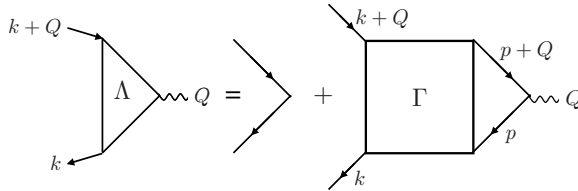


**Figure 2.** Structure of the vertex function  $\Lambda_Q$ . The spin fluctuation (wavy line) carries momentum  $\approx Q$ .  $\Gamma$  is the ph-irreducible four-point function

This small factor (at  $d = 3$ ) is avoided in those diagrams in which the external and internal momenta,  $k$  and  $p$  as in Fig. 2, are decoupled. The first such diagram (two-loop contribution) has three  $\chi$ 's, two of them coupled to  $\chi_E$  (see Fig. 3)

$$\Lambda_Q(k; Q) = u^6 \Lambda_Q^6 \Lambda_v^2 \int (dq) G(k - q) T(q; Q) \chi(Q + q) \chi_E(q) \quad (30)$$

where  $u \approx N_0^{-1}$  is the interaction vertex (we have altogether six endpoints of the spin fluctuation propagator, with one interaction vertex  $u$  each). We define the quantity (triangle loop on the right side of Fig. 3)

$$T(q; Q) = \int (dp) G(p - q) G(p + Q) G(p) \quad (31)$$

and approximate  $T(q; Q) \approx T(0; 0) \approx N_0/\epsilon_F$ . We now use

$$\text{Im}\chi(\mathbf{q} + \mathbf{Q}, \nu) = \frac{N_0|\nu|\Lambda_Q^2}{(q^2 + r)^2 + (|\nu|\Lambda_Q^2)^2} \quad (32)$$

where  $\nu$  and  $q$  are dimensionless (frequencies and wave vectors in units of  $\epsilon_F$  and  $k_F$ ), and from Eq. (18),

$$\text{Im}\chi_E(\mathbf{q}, \nu) = \frac{N_0^3 \Lambda_Q^{2d-3} (|\nu|)^{d-1/2}}{[q^2 + r + |\nu|\Lambda_Q^2]^{(d+1)/2}} \quad (33)$$

The imaginary part of the vertex function in the critical regime ( $r = 0$ ) is then approximately given by

$$\begin{aligned} \text{Im}\Lambda_Q(k; Q) &\propto \Lambda_Q^6 \Lambda_v^2 \int_0^\omega d\nu \int dq q^{d-2} \frac{\Lambda_Q^{2d-1} (|\nu|)^{d+1/2}}{[q^2 + r + |\nu|\Lambda_Q^2]^{\frac{d+5}{2}}} \\ &\propto \Lambda_v^2 \Lambda_Q^{2d-5} \int_0^\omega d\nu (|\nu|)^{d+1/2} \int_{\Lambda_Q \sqrt{|\nu|}} \frac{dq}{q^7} \\ &\propto \Lambda_v^2 \Lambda_Q^{2d-1} |\omega|^{d-3/2}. \end{aligned}$$

on the cold part of the Fermi surface (external particle and hole are both ‘‘cold’’). Here a factor of  $1/q$  was generated by the angular integration of the Green’s function, as in Eq. (8). A more complete account of this derivation may be found in Ref. [22]. The real part of  $\Lambda_Q(k; Q)$  is obtained by Kramers-Kronig transform. We add the bare value  $\Lambda_Q = 1$ , and find, on the cold part of the Fermi surface

$$\text{Re}\Lambda_Q(k; Q) = 1 + c_\Lambda \Lambda_v^2 \Lambda_Q^{2d-1} |\omega|^{d-3/2} + \dots \quad (34)$$

In the hot region we have (considering that only one of the external momenta will be at the hot spot, as discussed at the end of section III),

$$\text{Im}\Lambda_{Q,h} \propto \Lambda_v \Lambda_{v,h} \Lambda_Q^{2d-1} |\omega|^{d-3/2} \quad (35)$$

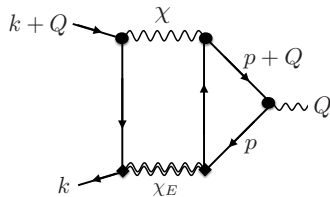


**Figure 3.** Two-loop diagram for  $\Lambda_Q$ . The black dots ( $\Lambda_Q$ ) and diamonds ( $\Lambda_Q^2 \Lambda_v$ ) signify the appropriate vertex functions [see Eq. (30)].

Here we take into account that the vertex  $\Lambda_{v,h}$  connected to the incoming hot quasiparticle or quasihole is generally different from the vertex  $\Lambda_v$  connected to the outgoing cold quasiparticles. Then, at the hot spots

$$\text{Re}\Lambda_{Q,h}(k; Q) = 1 + c_\Lambda \Lambda_{v,h} \Lambda_v \Lambda_Q^{2d-1} |\omega|^{d-3/2} + \dots \quad (36)$$

We see that  $\Lambda_Q$  depends on the position at the Fermi surface through the external vertex function factors  $\Lambda_v(\mathbf{k}; \mathbf{q})$ . In fact, even if we consider the self energy at a hot spot  $\mathbf{k}_h$ , only one of the incoming momenta, say  $\mathbf{k}$ , is hot, while the other one  $\mathbf{k} + \mathbf{q}$  (where  $\mathbf{q}$  is the momentum transferred to the energy fluctuation) is typically cold. Ward identities for vertex functions at non-zero  $\mathbf{q}$  are discussed in Ref. [22]. There it is shown that the full vertex (including reducible parts) is related to the  $Z$ -factors of the particle and hole lines by  $\Lambda_v(\mathbf{k}; \mathbf{q}) \approx \frac{1}{2}(Z_{\mathbf{k}}^{-1} + Z_{\mathbf{k}+\mathbf{q}}^{-1})$ . This property is expected to carry over to the irreducible vertex as well. We therefore conclude that  $\Lambda_v(\mathbf{k}_h; \mathbf{q}) \approx \Lambda_{Q,h} \approx \frac{1}{2}(Z_h^{-1} + Z^{-1})$  whereas for cold quasiparticles  $\Lambda_v(\mathbf{k}; \mathbf{q}) \approx Z^{-1}$ .

#### 4. Self-consistent determination of self energy and vertex functions

The expressions for the self energy and the vertex functions derived above form a set of self-consistent equations for  $Z^{-1}$ ,  $Z_h^{-1}$ , and  $\Lambda_Q, \Lambda_{Q,h}$ . We now discuss the solution of these equations in the limiting cases of weak and strong coupling. In the case of strong coupling we assume  $Z^{-1} \gg 1$  and  $\Lambda_Q \gg 1$ . We first consider the cold regions. Combining Eqs. (26,34), we find  $Z^{-1} = \Lambda_Q$  and hence

$$Z^{-1} \propto |\omega|^{-(d-3/2)/2d} = |\omega|^{-\eta} \quad (37)$$

which is the power law already found in Ref. [7] and from which  $\eta = (2d - 3)/4d$  as quoted earlier.

The weak coupling behavior is found as

$$\begin{aligned} Z^{-1} &= 1 + b_Z |\omega|^{d-3/2} \\ \Lambda_Q &= 1 + c_\Lambda |\omega|^{d-3/2} \end{aligned} \quad (38)$$

At the hot spots we have two contributions to the self-energy, and  $Z_h^{-1} = 1 + X_h + Y_h$ . By examining the powers of  $\omega$  and  $\Lambda$  in Eqs. (28,29), we determine that  $X_h \gg Y_h$ . The external momenta of the self-energy are by assumption at the hot spots, while the internal momenta of the Green's function (in  $\Sigma = \int \chi G$ ) are not, if we take typical values of the momentum  $\mathbf{q}$ . Then the vertex function at the hot spots Eq. (36) is obtained as

$$\Lambda_{Q,h} \propto (Z_h^{-1} + Z^{-1}) \quad (39)$$

If we substitute this  $\Lambda_{Q,h}$  for the vertex function in Eq. (29), we get

$$Z_h^{-1} = 1 + c'_Z (Z_h^{-1} + Z^{-1})^2 Z^{-d+3} |\omega|^{(d-3)/2} \quad (40)$$

At weak coupling, we find

$$Z_h^{-1} = 1 + c'_Z |\omega|^{(d-3)/2} \quad (41)$$

The behavior at strong coupling cannot be read off directly from the self-consistent equations. Inspection of Eq. (29) shows that  $Z_h^{-1} > Z^{-d+1}|\omega|^{(d-3)/2} > |\omega|^{-(\frac{1}{4}+\frac{3}{4d})}$ . The exponent  $\eta = (\frac{1}{4} + \frac{3}{4d}) > \frac{1}{2}$  implies that quasiparticles are no longer well-defined at the hot spots in the strong coupling regime. As explained in Sec. II,  $\eta$  less than about 0.36 is required. Within our approach, which assumes the existence of well-defined quasiparticles, we are not equipped to describe the properties of incoherent fermionic excitations at the hot spots. As long as the extension of the hot spots is sufficiently small, their contribution to the thermodynamic and transport properties may be expected to be small, too. We will therefore discard the effect of hot quasiparticles in the following.

## 5. Renormalization group flow

The analysis of the previous paragraphs reveals that for sufficiently strong interactions, the low-energy properties of a system near a metallic quantum critical point is governed by new scaling behavior. As we discussed in the previous section, the limiting cases of strong and weak coupling may exhibit different power-law (scaling) exponents as  $\omega \rightarrow 0$ . It is a natural question to ask whether this behavior can be expressed in terms of renormalization group (“RG”) equations involving corresponding  $\beta$ -functions that determine the renormalization group flow of the self energies of hot and cold quasiparticles. We shall express the RG flow in terms of dimensionless “coupling constants”,  $\alpha_h$  and  $\alpha_c$  that are related to the self energies for the hot and cold regions

$$\frac{d\alpha_l}{d \log(\epsilon_F/|\omega|)} = \beta_l(\alpha_c, \alpha_h). \quad (42)$$

with  $l \in \{h, c\}$ . As suggested by us previously in Ref. [7], a natural definition of the dimensionless coupling constants is in terms of the  $Z$ -factor:  $\alpha_l = Z_l^{-1} - 1$ .

To consider the associated renormalization group flow for cold particles we use  $\alpha_c$  with the results of Sec. III for the self energy. The scaling quantity is  $\alpha_c(t)$  as a function of  $t = \ln(\epsilon_F/|\omega|)$ . It is given by [see Eq. (26)]

$$\alpha_c = b_Z(1 + \alpha_c)^{2d+1}e^{-(d-3/2)t} \quad (43)$$

Taking the derivative of  $\alpha_c$  with respect to  $t$ , we get

$$\frac{d\alpha_c}{dt} = -(d-3/2)\alpha_c + (2d+1)\frac{\alpha_c}{1+\alpha_c}\frac{d\alpha_c}{dt} \quad (44)$$

Solving for  $d\alpha_c/dt$ , we find the flow equation

$$\frac{d\alpha_c}{dt} = \beta_c(\alpha_c) = \frac{-(d-3/2)\alpha_c(1+\alpha_c)}{1-2d\alpha_c}. \quad (45)$$

The  $\beta$ -function for cold quasiparticles only depends on the coupling constant  $\alpha_c$  itself.

For weak coupling,  $\alpha_c \ll 1$ ,

$$\beta_c(\alpha_c \ll 1) \approx -\left(d - \frac{3}{2}\right)\alpha_c, \quad (46)$$

*i.e.* for  $d > \frac{3}{2}$  the interaction between cold carriers is irrelevant and the flow of  $\alpha_c$  is directed towards the stable fixed point at  $\alpha_c = 0$ . In the neighborhood of this fixed point one finds

$$\alpha_c \propto |\omega|^{d-3/2}, \quad \alpha_c \ll 1/(2d), \quad (47)$$

This corresponds to subleading corrections to Fermi liquid scaling, in full agreement with the results found by Hartnoll et al.[26] for  $d = 2$ . For weak coupling, deviations from Fermi-liquid physics are limited to hot portions of the Fermi surface (see below). For  $d > 2$  it is furthermore possible to integrate out the fermionic degrees of freedom (see Ref. [24]) and one recovers the physics described by the Hertz-Millis-Moriya theory.

For large values of the coupling constant we obtain

$$\beta_c(\alpha_c \gg 1) \approx \frac{d-3/2}{2d}\alpha_c. \quad (48)$$

Now, the system flows to strong coupling,  $\alpha_c \rightarrow \infty$ ; it diverges according to a power law

$$\alpha_c \propto |\omega|^{-\eta}, \quad \alpha_c \gg \alpha_c^* \quad (49)$$

with same anomalous exponent as determined from the self consistency argument discussed above:

$$\eta = \frac{d-3/2}{2d}. \quad (50)$$

The threshold value of the coupling constant that separates conventional and critical Fermi liquid behavior is  $\alpha_c^* = 1/(2d)$ , where the  $\beta$ -function has a pole. It defines a separatrix that distinguishes the scaling in the strong and weak coupling regimes. While a pole in the  $\beta$ -function is rather unusual, it is not without precedent. A prominent example is the instanton-based derivation of the  $\beta$ -function of supersymmetric Yang-Mills theories in Ref. [27]. Whether the pole in  $\beta(\alpha)$  of our theory is a robust phenomenon or will be smoothed is unclear at this point. If smoothed, conventional and critical Fermi liquid behavior would be separated by an unstable fixed point at  $\alpha_c^* = 1/2d$ , where  $\beta$  changes sign. Thus, if one increases the value of the coupling constant, right at the antiferromagnetic quantum critical point, the system passes through yet another quantum critical point that separates conventional and unconventional behavior. This is illustrated in Fig. 4

## 6. Scaling of dynamic and thermodynamic quantities

In this section we discuss the observable quantities as calculated with our theory in the strong coupling regime, making use of the results derived in the earlier sections. We recall that the contribution from hot quasiparticles is expected to be small. While the results below have been published before, for the most part the presentation given here is somewhat different. We also review the comparison of our results with experimental findings for two of the quantum critical heavy fermion compounds, YbRh<sub>2</sub>Si<sub>2</sub> (YRS) and CeCu<sub>6-x</sub>Au<sub>x</sub> at  $x = 0.1$  (CCA), which we believe to be described well by the strong coupling theory.

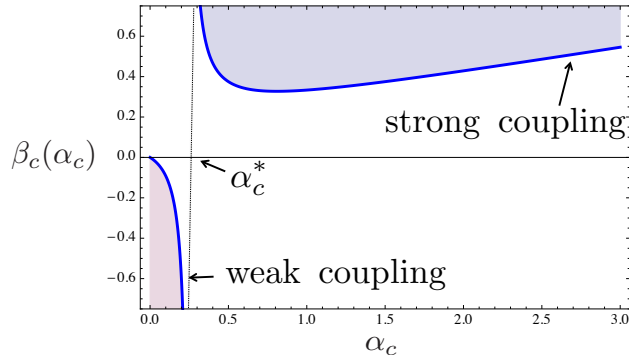


**Figure 4.**  $\beta$ -function of the renormalization group flow of cold quasiparticles for  $d = 2$ . While the flow is towards weak coupling if  $\alpha_c < \alpha_c^*$ , the system flows to infinite coupling with power law behavior for  $\alpha_c > \alpha_c^*$ . The two regimes, corresponding to weak and strong coupling, are separated by a pole of the  $\beta$ -function.

The spin fluctuations in  $\text{YbRh}_2\text{Si}_2$ , as studied by neutron scattering [28] show two components: a three-dimensional ferromagnetic component in a somewhat higher temperature range,  $0.3 \text{ K} < T < 10 \text{ K}$ , that gives rise to non-Fermi liquid behavior and an incommensurate antiferromagnetic component below  $T \approx 0.3 \text{ K}$ , which is presumably responsible for the quantum critical behavior observed at the field-tuned QCP. The critical field is low,  $H_c \approx 60 \text{ mT}$  and the AFM critical temperature is also low,  $T_N(H = 0) \approx 70 \text{ mK}$ , well separated from the Kondo scale of  $T_K \approx 20 \text{ K}$  estimated for this heavy fermion compound. As the system is cooled down in the critical field, the ferromagnetic fluctuations cause a logarithmically increasing effective mass (or equivalently  $1/Z$ ), as observed experimentally taking the system into the strong coupling domain (as discussed at the beginning of Sec. IV), when the low temperature regime dominated by antiferromagnetic fluctuations is reached.

For  $\text{CeCu}_{6-x}\text{Au}_x$  the spin fluctuations have been studied in much more detail (large crystals, no neutron absorbing elements). Quasi-two-dimensional critical incommensurate antiferromagnetic fluctuation[29, 30] are found and in addition, two-dimensional ferromagnetic fluctuations.[31] We remark that the hot regions of the Fermi surface generated by quasi-two-dimensional antiferromagnetic fluctuations in a three-dimensional metal are extended, i.e. cover a non-zero region of the Fermi surface. Both of these fluctuations may be expected to drive the system into the strong-coupling regime of a quasi-two-dimensional critical antiferromagnetic system as we considered above.

In the following we report the comparison of the theoretical result for each observable considered with available experimental data for the two compounds, YRS and CCA. Such comparisons were illustrated with figures in our earlier papers on the subject; these are cited in the appropriate places.

In Fig. 5, we give a sketch of a quantum critical phase diagram which identifies the various regions to which we refer below in our comparisons to data,



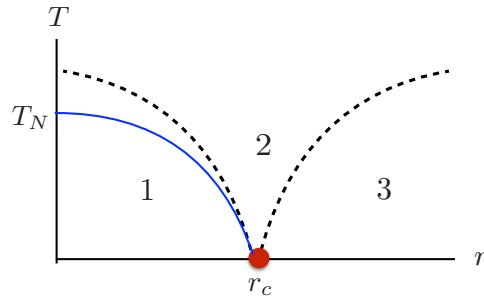


**Figure 5.** Sketch of example quantum critical phase diagram. Temperature  $T$  vs control parameter  $r$ .  $r_c$  marks the quantum critical point. Region 1: ordered regime, *e.g.* antiferromagnet, with Néel temperature  $T_N$  at  $r = 0$ . Region 2: quantum critical regime. Region 3: quantum disordered regime, often a paramagnetic Fermi liquid region. Dashed lines represent crossovers into the quantum critical regime. Blue line represents the thermodynamic Néel transition into the antiferromagnetic state.

### 6.1. Correlation length of bosonic fluctuations and dynamical scaling

We begin by discussing the correlation length  $\xi$  of spin fluctuations, which is identical to the one of energy fluctuations. Here and in the following, we only consider the strong-coupling regime. It follows from Eq. (6) that  $\xi = \xi_0 r^{-1/2}$ . The renormalized control parameter  $r$  is scale dependent; it depends on temperature  $T$  and frequency  $\nu$ , and its limiting value  $\lim_{\{T,\nu\} \rightarrow 0} r \equiv r(0)$ . In the critical regime (region 2 of Fig. 5), *i.e.* when we may put  $r(0) = 0$ , the scaling may be read off Eq. (6) as  $\xi(T, \omega) \propto [\max\{T, \omega\}]^{-1/z}$ . Here  $z$  is the dynamic critical exponent, obtained by determining the scaling relation  $\nu \propto q^z$  from the denominator of Eq. (6). By using the scaling results of previous sections for  $\Lambda_Q \sim Z^{-1} \propto |\omega|^{-\eta}$ , one finds

$$z = 2/(1 - 2\eta) = 4d/3. \quad (51)$$

It remains to determine the scaling of the correlation length with an external field representing the control parameter. For definiteness we consider a magnetic field tuned quantum phase transition in the following. The divergence of the correlation length at  $\{T, \omega\} \rightarrow 0$ , as a function of  $H$ , is by definition given as  $\xi(H) \propto r_0^{-\nu}$ , where  $r_0 = |H/H_c - 1|$ . The correlation length exponent  $\nu$  may be determined as follows. We know that  $r(0)$  must vanish at the QCP as a power of  $r_0$ , which in general is not linear, for the following reason. A uniform magnetic field  $H$  couples to the system via the spin density of conduction electrons. The corresponding coupling constant is critically renormalized near the QCP, as represented by a three-legged vertex  $\Lambda$ , in the limit momentum  $q \rightarrow 0$ . This vertex is known to be equal to  $1/Z$ , by virtue of the usual Ward identity. We thus have  $r(0) \propto r_0/Z$ . The scaling of  $Z$  with  $|H - H_c|$  may be derived from the scaling of  $Z$  with  $\omega$ ,  $Z \propto \omega^\eta$ , by noting that the two scaling relations for  $\xi$ , inside and outside the critical cone, have to match at the crossover, implying  $\omega \propto r_0^{\nu z}$ . It follows that  $r(0) \propto \xi^{-2}(H) \propto r_0^{1-\eta\nu z}$ , from which one finds the correlation

length exponent as

$$\nu = 2/(2 + z\eta) = 3/(3 + 2d) \quad (52)$$

To summarize, the inverse correlation length (in units of  $k_F$ ) may be expressed as

$$\xi^{-1}(T, H) \propto T^{1/z} + c_\xi r_0^\nu \quad (53)$$

with  $T$  in units of  $\epsilon_F$  and  $c_\xi$  a constant of order unity. The above discussion applies as well to the case of tuning by pressure, where  $r_0 = |p/p_c - 1|$ , or chemical composition, where  $r_0 = |x/x_c - 1|$ , in which cases the corresponding particle density vertex is likewise critically renormalized by a factor  $1/Z$ .

In Ref. [7], we developed the scaling of the spin fluctuation spectral function; it shows the following general scaling behavior:

$$\text{Im } \chi(\mathbf{q}, \omega) \propto T^{-2/z} \Phi_\chi\left(\frac{\omega}{T}, q\xi, r_0 T^{1/z\nu}\right) \quad (54)$$

where the scaling function is given as [7]

$$\Phi_\chi(x, u, w) = \frac{x(x^2 + a^2)^{-\eta}}{(1 + w^{2\nu})[1 + u^2] + [x(x^2 + a^2)^{-\eta}]^2} \quad (55)$$

Here, the constant  $a$  mediates the relation between energy scales  $\omega$  and  $T$ . *e.g.*  $\omega^\gamma \rightarrow (\omega^2 + a^2 T^2)^{\gamma/2}$ . In the critical regime, where we may put  $r_0 = 0$ , the function  $T^{2/z} \text{Im}\chi(\mathbf{q}, \omega)$  obeys  $\omega/T$ -scaling.

The dynamical scaling near the QCP of  $\text{CeCu}_{6-x}\text{Au}_x$  at  $x = 0.1$  has been studied using inelastic neutron scattering.[29, 30] In this material, the antiferromagnetic spin fluctuations appear to be quasi-two-dimensional. In the critical regime ( $r_0 = 0$ ) the data obey  $\omega/T$ -scaling, of the form shown in Eq. (55), where the exponent  $\eta$  has been determined as  $\eta_{ex} \approx 0.1 - 0.15$ , while our theory gives  $\eta_{th} = 1/8 = 0.125$ . A detailed comparison of experiment and theory, showing very good agreement, is given in Ref. [7].

## 6.2. Free energy

The critical behavior of the free energy may be derived from the critical behavior of the fermionic quasiparticles by expressing the free energy density in terms of the fermionic self-energy

$$f(T, r_0) = \frac{1}{2\pi} \int_0^T dT' N_0 \int \frac{d\omega}{(T')^2 \cosh^2(\omega/2T')} \int d\Omega_{\mathbf{k}} [\omega - \Sigma(\mathbf{k}_F, \omega)] \quad (56)$$

where  $\int d\Omega_{\mathbf{k}}$  is a normalized angular integral over the Fermi surface. It may be shown that the contribution of the bosonic fluctuations to the free energy is subleading. Substituting the results for  $\Sigma$  obtained above, we find that in the strong-coupling regime,  $f$  obeys the scaling

$$f(T, r_0) = \xi^{-(2d+1)} \Phi_f(r_0 \xi^{1/\nu}, T \xi^z) \quad (57)$$

This may be rewritten as

$$f(T, r_0) = T^{(2d+1)/z} \Psi(r_0^{z\nu}/T) \quad (58)$$

where the exponent of the prefactor may be expressed as  $(2d + 1)/z = 2 - \eta$

$$\Psi(x) \propto [1 + c_f x^\eta]^{-1} \quad (59)$$

where  $c_f$  is a constant of order unity, and the second term in the square brackets ensures that  $f(T, H) \propto T^2$  in the Fermi liquid regime, where  $x \gg 1$ . In Eq. (57) the "correlation volume" enters as  $\xi^{2d+1}$  rather than  $\xi^{d+z}$ . This is a consequence of the fact that the dominant critical degrees of freedom are the fermionic ones. It may be shown that  $\xi^{2d+1} = \xi_f^{d_f+z_f}$ , with the fermionic correlation length given by  $\xi_f^{-1} \propto T/Z(T) \propto T^{1-\eta}$ , which grows much faster than the bosonic counterpart  $\xi^{-1} \propto T^{1/z}$ . The fermionic dimension  $d_f = 1$  and the fermionic dynamical exponent  $z_f = 1/(1 - \eta)$ . The fermionic correlation length exponent  $\nu_f = 1$ . In the literature on quantum critical phenomena in metals the bosonic correlation length  $\xi$  is usually presented as the relevant length scale and we follow this usage.

Taking derivatives of the above free energy expressions, we may derive the critical behavior of thermodynamic quantities. We start with the specific heat coefficient  $\gamma = C/T$ , found as the second derivative of  $f$  with respect to temperature:

$$C(T, r_0)/T \propto r_0^{-(2d-3)/(2d+3)} + c_\gamma T^{-(2d-3)/4d}. \quad (60)$$

This implies that  $C/T$  diverges in dimensions  $d = 3, 2$  as a power law, both when approaching the QCP at  $r_0 = 0$  as  $T \rightarrow 0$  or else at  $T = 0$  as  $r_0 \rightarrow 0$  from the Fermi liquid phase.

In the quantum critical regime,  $r_0 = 0$ , one thus finds for  $3d$  and  $2d$  fluctuations,  $C/T \propto T^{-1/4}$  and  $C/T \propto T^{-1/8}$ , both in good agreement with the data on YRS[32, 5] and on CCA,[33, 7] respectively. In the case of YRS, a classical contribution  $C/T \propto 1/T$  was included; it may be traced to the excitation of spin resonance bosons [21] of energy lower than the lowest  $T$  accessible in experiment. Approaching the QCP from the Fermi liquid side our theory predicts  $C/T \propto r_0^{-1/3}$  for  $3d$ -fluctuations, in excellent agreement with data on YRS.[34, 42]

Next we calculate the magnetization  $M = -\partial f/\partial H = -\partial f/\partial r_0$  and find:

$$M(T, H) - M(0, H_c) \propto -r_0^{2d/(2d+3)} - c_M T \quad (61)$$

which represents nonanalytic (cusp-like) behavior, as the QCP is approached. In the critical regime the linear  $T$ -law amended by a Fermi liquid  $T^2$ -component has been shown to account well for the YRS-data [35, 6] and the CCA-data.[33, 7]

The magnetic susceptibility is given by a further derivative with respect to  $r_0$ :

$$\chi(T, H) - \chi(0, H_c) \propto -r_0^{(2d-3)/(2d+3)} - c_\chi T^{(2d-3)/4d}, \quad (62)$$

which as a function of either  $T$  or  $H$  shows a downward cusp. In the critical regime, and for  $d = 3$  we find the power law  $T^{1/4}$ , which, when augmented by the Fermi liquid  $T^2$  component, accounts very well for the data on YRS. [36, 6]

A quantity of special interest is the Grüneisen ratio, defined as the ratio of entropy derivatives

$$\Gamma_G = -\frac{(\partial S/\partial X)_T}{T(\partial S/\partial T)_X} \quad (63)$$

where  $X$  denotes a control parameter field. For concreteness we consider the case, appropriate for YRS,  $X = H$ , where  $H$  is an applied magnetic field, in the following. Then, the magnetic Grüneisen ratio is

$$\Gamma_G = -\frac{\partial M/\partial T}{T(\partial S/\partial T)_H} = \begin{cases} -G_r/|H - H_c|, & T \rightarrow 0 \\ c_\Gamma T^{-(2d+3)/4d}, & H \rightarrow H_c. \end{cases} \quad (64)$$

Here we find universal behavior in the Fermi-liquid regime, with the coefficient  $G_r = -\nu[z - (2d + 3)/3] = -\nu_f(z_f - d_f)$ , in agreement with the result following from a phenomenological analysis that assumes hyperscaling.[37] The magnetic Grüneisen ratio has been experimentally determined for YRS[35]to follow a  $T^{-0.7}$ -law in the critical regime, and a coefficient  $G_r \approx -0.3$  in the Fermi liquid regime. This compares well with the theoretical results [6]  $T^{-3/4}$  and  $G_r = -1/3$ . In CCA,  $\Gamma_G$  appears to grow logarithmically with decreasing temperature, and hence much slower than the predicted  $T^{-7/8}$ -law. The coefficient  $G_r$  has not yet been determined.[3]

### 6.3. Transport and relaxation properties

The basic inelastic relaxation rate is obtained from the imaginary part of the self-energy. As discussed in Sec. II, the quasiparticle relaxation rate is defined as  $\Gamma = Z \text{Im}\Sigma$ ; it obeys the scaling law[6]

$$\Gamma = \xi^{-z} \Phi_\Gamma(r_0 \xi^{1/\nu}, T \xi^z) \quad (65)$$

which may be reexpressed as

$$\Gamma(T, H) = T \Psi_\Gamma(r_0^{z\nu}/T) \quad (66)$$

with

$$\Psi_\Gamma(x) \propto [1 + c_\Gamma x]^{-1} \quad (67)$$

The critical behavior of the electrical resistivity  $\rho(T, H)$  may be obtained in the limit of low temperatures, where the contribution of inelastic processes is small, so that the elastic scattering contribution  $\rho(0, H)$  dominates. Then we may write

$$\rho(T, H) - \rho(0, H_c) \propto \langle q^2 \rangle \Gamma / Z \quad (68)$$

The factor  $\langle q^2 \rangle$  accounts for vertex corrections, and is approximately given by the typical momentum transfer in a scattering process squared. Under the assumption made above that impurity scattering dominates, the relevant inelastic processes are dressed by elastic processes such that the typical momentum transfer is  $k_F$ , and is thus noncritical. In this case we may put  $\langle q^2 \rangle \approx c_{imp} k_F^2$ , where  $c_{imp}$  is the impurity concentration. We then find

$$\rho(T, H) - \rho(0, H_c) \propto c_{imp} \begin{cases} T^{1-\eta}, & H \rightarrow H_c \\ T^2 |H - H_c|^{-(3z/2-1)\nu}, & T \rightarrow 0. \end{cases} \quad (69)$$

In the opposite case of clean samples (but still in the regime  $\rho(T, H)/\rho(0, H_c) - 1 \ll 1$ ) the typical momentum transfers are small,  $\langle q^2 \rangle \propto T/Z^2 \propto T^{1-2\eta}$  in the critical regime and  $\propto T|H/H_c - 1|^{-2(2d-3)/(2d+3)}$  in the Fermi liquid regime. We find

$$\rho(T, H) - \rho(0, H_c) \propto \begin{cases} T^{2-3\eta}, & H \rightarrow H_c \\ T^3/|H - H_c|, & T \rightarrow 0 \end{cases} \quad (70)$$

In the case of YRS (3d spin fluctuations), we then expect  $\rho(T, H) - \rho(0, H_c) \propto c_{imp}T^{3/4}$ , in good agreement with experiment.[39, 5] A comparison of the data in Refs. [39, 5] with those of somewhat dirtier samples [40] shows that the prefactor of the  $T^{3/4}$ -law indeed appears to grow with impurity concentration. For CCA ( $d = 2$ ),  $\text{CeCu}_{6-x}\text{Au}_x$ , for  $x = x_c = 0.1$ , we find  $c_{imp}T^{7/8}$  in reasonable agreement with the data of Ref. [38]. These data were previously fit by a linear  $T$  law, which describes the data almost as well. AFM order is found for  $x \geq 0.15$  but the  $T_N$  can be tuned to zero by hydrostatic pressure ( $p_c \approx 5$  kbar) or magnetic field ( $H_c \approx 0.4$  T).[41] It was found that for pressure tuning, the critical behavior of the resistivity follows an approximately linear  $T$ -law, in agreement with the behavior found at the critical concentration  $x = 0.1$ . However, the  $\rho$  data obtained by magnetic field tuning showed a  $T^{3/2}$ -law, as is expected for a weak-coupling spin density wave QCP. The contrast is instructive: it shows that for CCA with  $x = 0.2$ , both strong (pressure tuning) and weak (field tuning) coupling critical behavior may occur. We may interpret this within our theory with the conjecture that the magnetic field of  $H_c \approx 0.4T$  needed to reach the QCP suppresses the magnetic fluctuations thought to be necessary to get into the strong coupling regime. In this study,[41] it was also found that the prefactor of the  $T$ -law appeared to increase with disorder.

The dynamical conductivity  $\sigma(\omega + i0)$  may be represented as

$$\sigma(\omega + i0) = \frac{\omega_p^2}{4\pi} \frac{i}{\omega - M(\omega + i0)} \quad (71)$$

where  $\omega_p^2 = 4\pi e^2 n/m$  is the plasma frequency squared and  $M(\omega + i0)$  is the relaxation kernel.  $\sigma(\omega + i0)$  at not too high frequencies,  $\omega \ll \epsilon_F$ , follows, using  $\omega - M(\omega + i0) = \omega Z(\omega) + i/\tau(\omega)$ , where  $Z(\omega) = 1 - \text{Re}M(\omega)/\omega$  and  $1/\tau(\omega) = -\text{Im}M(\omega)$  as

$$\frac{\omega_p^2}{4\pi} \frac{\tau(\omega)(1 + i\omega\tau(\omega)Z(\omega))}{1 + [\omega Z(\omega)\tau(\omega)]^2} \quad (72)$$

We note that  $Z(\omega)$  may be interpreted as inverse effective mass ratio  $Z = m/m^*$ .

If we neglect vertex corrections we may relate  $M$  to the self energy  $\Sigma$  as

$$M(\omega + i0) = 2\Sigma(\omega + i0) + i/\tau_{imp} \quad (73)$$

where  $\tau_{imp}$  is the momentum relaxation time due to impurity scattering.

Near a quantum critical point and in the critical regime (control parameter  $r_0 = 0$ ) we expect the scaling behavior of the effective mass ratio

$$Z(\omega, T; r = 0) \propto T^\eta \Phi_Z(|\omega|/T, r = 0), \quad (74)$$

$$\Phi_Z(x, 0) \propto x^\eta, \quad x \gg 1$$

$$\Phi_Z(x, 0) = 1, \quad x \ll 1$$

and of the relaxation rate

$$\tau^{-1}(\omega, T; r = 0) = c_{in} T^{1-\eta} \Phi_\tau(|\omega|/T, r = 0) + 1/\tau_{imp}, \quad (75)$$

$$\Phi_\tau(x, 0) \propto x^{1-\eta}, \quad x \gg 1$$

$$\Phi_\tau(x, 0) = 1, \quad x \ll 1$$

where  $\eta$  is the critical exponent introduced in Sec. IV, Eq. (37). A simple interpolation formula for the  $\Phi$ 's would be

$$\Phi_Z(x; 0) = 1 + c_Z x^\eta,$$

$$\Phi_\tau(x; 0) = 1 + c_\tau x^{1-\eta} \quad (76)$$

Near the critical point and in the quantum disordered regime, at  $T = 0$  and non-zero but small  $r$ , we have for  $Z$

$$\begin{aligned} Z(\omega, T = 0; r) &\propto r^{(1-z/2)\nu} \Phi_{Zr}(|\omega|r^{-\nu z}; r\xi^{1/\nu} = 1), \\ &\propto r^{(1-z/2)\nu} \end{aligned} \quad (77)$$

and for the relaxation rate

$$\begin{aligned} \tau^{-1}(\omega, T = 0; r) - \tau_{imp}^{-1} &\propto r^{(1+z/2)\nu} \Phi_{\tau r}(|\omega|r^{-\nu z}; 1) \\ &\propto \omega^2 r^{-(3z/2-1)\nu}, \end{aligned} \quad (78)$$

where  $\nu$  is the correlation length exponent and  $z$  is the dynamical exponent. Here, at non-zero temperature,  $|\omega|$  should be replaced by [as in Eq. (55)]  $[\omega^2 + aT^2]^{1/2}$ , where  $a$  is a constant of order unity.

The thermopower in the limit of low temperatures, when impurity scattering dominates, is given in terms of the conductivity  $\sigma_{imp}(\mu)$  at chemical potential  $\mu$  by

$$S = \frac{\pi^2 T}{3e} \frac{\partial \ln \sigma_{imp}(\mu)}{\partial \mu} \propto T \frac{m^*}{m} \quad (79)$$

Here we have used the fact that  $\sigma_{imp}(\mu)$  does not depend on the renormalized effective mass, but  $\mu = k_F^2/2m^*$  such that  $\partial \ln \sigma_{imp}/\partial \mu = (\partial \ln \sigma_{imp}/\partial k_F)(m^*/k_F)$ . An experimental study of the thermopower of YRS[42] shows a power law behavior of  $S$  in the critical regime,  $S \propto T^{3/4}$ , just as predicted by our theory [6]. In the Fermi liquid regime, where our theory predicts  $S/T \propto |H - H_c|^{-1/3}$ , experiment does show a somewhat weaker increase of  $S/T$  as  $H \rightarrow H_c$ . [42]

The nuclear spin relaxation rate is governed by the local electronic spin fluctuation spectrum:

$$\begin{aligned} \frac{1}{T_1 T} &\propto \left[ \frac{1}{\omega} \int (dq) \text{Im} \chi(q, \omega) \right]_{\omega \rightarrow 0} \\ &\propto \frac{1}{Z^2(\omega = 0)} \xi^{4-d} \end{aligned} \quad (80)$$

where  $\xi^{-1} \propto T^{1/z} + c_\xi |H - H_c|^{\nu\eta}$ . In the critical regime one finds  $1/T_1T \propto T^{-(d+6)/4d}$ , and in the Fermi liquid regime we get  $1/T_1T \propto |H - H_c|^{-\nu\eta(5d+12)/3}$ . An experimental study of the nuclear spin relaxation rate[43] in YRS shows  $1/T_1T \propto T^{-\alpha_N}$ , with  $\alpha_N > 1/2$ . The lowest field in this experiment is about twice the critical field  $H_c \sim 0.06$  T so outside the critical region. Our theory prediction is  $1/T_1T \propto T^{-3/4}$ . [44] A more recent NMR study of YRS using magnetic field oriented parallel to the c-axis revealed a puzzling two-component signal [45], one component showing critical behavior, while the other has Fermi liquid characteristics.

## 7. Summary and Conclusion

We have reviewed the theory of critical quasiparticles in the context of the properties of a metallic system in the neighborhood of an antiferromagnetic quantum critical point. We discussed the conditions under which a coherent quasiparticle description may be used to analyze the behavior of metallic electrons in the critical region where their effective mass diverges as a consequence of the interaction of the fermions with the bosonic critical quantum fluctuations. The essential ingredient of the theory is accounting for the fact that due to this interaction, both the fermions and the bosons become critical; this leads to self-consistent conditions for the electron self energy and various vertex amplitudes that renormalize the interaction between the fermions and the critical fluctuations.

The self-consistent equations have a “weak-coupling” solution that reproduces the conventional picture established decades ago in works by Hertz, Millis, Moriya and reviewed in various places. However there are also strong-coupling solutions in the low temperature (or excitation frequency) regime that lead to new power laws for thermodynamic and transport properties in the critical region.

When the ordered phase has a spatial variation characterized by an ordering wave vector  $\mathbf{Q}$ , as is the case for charge or spin density wave order, then there may be special regions of the Fermi surface that are connected by order parameter fluctuations of wave vector  $\mathbf{Q}$ . These are the so-called “hot spots”. In the general case of incommensurate antiferromagnetic quantum criticality, the interaction of the fermions with a single antiferromagnetic spin fluctuation (“one-loop” analysis) leads to a highly anisotropic electron self energy that has singular behavior only at the hot regions of the Fermi surface. However, the coupling to two spin fluctuations (“two-loop” analysis), which amounts to a critical energy fluctuation, may involve a total wave vector transfer  $\mathbf{q} \approx 0$ ; this gives singular behavior over the entire Fermi surface. This is the situation we have considered in the present work. Nevertheless, as a consequence of the internal structure of the interaction vertex of fermions with the energy fluctuation bosons, the hot and cold regions of the Fermi surface behave differently. We have analyzed the extent of the hot regions and we have shown that in the strong-coupling regime, there are no coherent critical quasiparticles in that part of the Fermi surface. The contributions of the incoherent parts of the electron spectrum to thermodynamics and transport are expected to be small and non-singular, so we have concentrated on the effects of the

singular critical quasiparticles that live at the cold regions.

From an examination of the self-consistent expressions for the cold quasiparticles, it is evident that there is different scaling behavior in the strong and weak coupling limits. We made this explicit by a renormalization group analysis for the flow of an appropriately chosen “coupling constant” that is determined by the self energy of the cold quasiparticles.

The derived properties of the critical quasiparticles in the strong-coupling regime determine the critical behavior of various transport and thermodynamic quantities. In preparation for the discussion of the experimental consequences of our theory of critical quasiparticles, we extracted, from the self-consistent analysis, the dynamical critical exponent  $z$  and the correlation length exponent  $\nu$  of the critical bosonic (spin) fluctuations. These enter the expressions for the spin fluctuation spectrum and the free energy in the quantum critical region; we reviewed the corresponding dynamical scaling form for both. From the free energy, we derived the critical behavior of thermodynamic quantities: the specific heat, the magnetization, the magnetic susceptibility, and the magnetic Grüneisen ratio. We reviewed the comparison of our theoretical results for these and also the spin fluctuation spectrum (as measured by inelastic neutron scattering) with the available data on two heavy-fermion compounds, YbRh<sub>2</sub>Si<sub>2</sub> (YRS) and CeCu<sub>6-x</sub>Au<sub>x</sub> at  $x = 0.1$  (CCA), both of which exhibit quantum critical behavior.

From the scaling behavior of the electron self energy, we gave the critical behavior of transport quantities: resistivity, magnetoresistivity, dynamical conductivity, thermopower, and NMR relaxation rate. Where data for YRS and/or CCA are available, the theory gives an excellent description. All of the comparisons of theory and experiment for YRS and CCA are described and illustrated with figures in Refs. [5, 6] (YRS) and Ref. [7] (CCA).

## Acknowledgments

We acknowledge useful discussions with H. v. Löhneysen, P. Gegenwart, J.D. Thompson, F. Ronning, Q. Si, C. M. Varma, and especially A.V. Chubukov and R. Fernandes. Part of this work was performed during the summers of 2014-16 at the Aspen Center for Physics, which is supported by NSF Grant No. PHY-1066293. J.S. and P.W. acknowledge financial support by the Deutsche Forschungsgemeinschaft through Grant No. SCHM 1031/4-1. %endacknowledgments

## Appendix A. Higher order contributions to $\Sigma$

In order to probe the validity of the two-loop result for the self energy of Sec. IIA2, we now estimate two higher order diagrams, containing two energy fluctuation propagators, in parallel and crossed:

$$\text{Im}\Sigma^{2E}(k) = \lambda_{2E}^2 \int (dq_1) \int (dq_2) G^t(k + q_1) G^{\bar{t}}(k - q_2) \quad (\text{A.1})$$



$$\begin{aligned}
& \times \text{Im}G(k + q_1 - q_2)\text{Im}\chi_E(q_1)\text{Im}\chi_E(q_2) \\
& \times \{b(\nu_1)(1 + b(\nu_2))(1 - f(\omega + \nu_1 - \nu_2)) + \\
& + (1 + b(\nu_1))b(\nu_2)f(\omega + \nu_1 - \nu_2)\}
\end{aligned}$$

Here  $G^t, G^{\bar{t}}$  are the time-ordered and anti-time-ordered Green's functions and  $\lambda_{2E} = \Lambda_v^3 \Lambda_Q^4$ , where an additional factor of  $\Lambda_v \propto Z^{-1}$  arises from a vertex correction straddling the two endpoints of  $\chi_E$  on each side of the diagram. The angular integrations of  $G^t, G^{\bar{t}}$  produce factors of  $1/q_{1,2}$ . Using  $\Lambda_Q \propto Z^{-1}$ , we find

$$\text{Im}\Sigma^{2E}(\mathbf{k}, \omega) = Z^{-14} \int_0^\omega d\nu_1 \int_0^{\nu_1} d\nu_2 \int dq_2 q_2^{d-2} \quad (\text{A.2})$$

$$\times \text{Im}\chi_E(\mathbf{q}_2, \nu_2) \int dq_1 q_1^{d-2} \text{Im}\chi_E(\mathbf{q}_1, \nu_1) \quad (\text{A.3})$$

The  $q$ -integrals may be done to give

$$\int dq_1 q_1^{d-2} Z^{-6} \text{Im}\chi_E(\mathbf{q}_1, \nu_1) \propto \frac{\nu_1^{d-3/2}}{Z^{2d+1}} \quad (\text{A.4})$$

Finally the frequency integrals may be performed with the result

$$\text{Im}\Sigma^{2E}(\mathbf{k}, \omega) \propto \frac{\omega^{2d-1}}{Z^{4(d+1)}} \propto \omega^{2d-1-4(d+1)\eta} \quad (\text{A.5})$$

which, compared with the one-loop result  $\omega^{1-\eta}$  is seen to be smaller by a factor  $\omega^{1-3\eta}$ . We recall that  $1 - 3\eta > 0$  for dimensions  $3/2 < d < 9/2$ , which means that the higher terms are irrelevant in dimensions  $d = 2, 3$ .

## Appendix B. Vertex corrections from single spin/energy fluctuation exchange

### Appendix B.1. Single spin fluctuation diagram

The relevant diagrams involve spin fluctuation propagators connected by single-particle Green's functions in such a way that the total momentum is  $\mathbf{Q}$ . The simplest diagram is the one with a single  $\chi(\mathbf{q}, \nu)$  crossing as in Fig. 2 with  $\Gamma$  replaced by  $\chi$ .

$$\begin{aligned}
\Lambda_{Q,h}^{(a)}(\mathbf{k}_h, \omega; \mathbf{Q}, \Omega \rightarrow 0) &= u^2 \Lambda_Q^2 \int (dq) G(k + q - Q) \\
&\times G(k + q) \chi(q + Q) \\
&\propto \Sigma^{(a)}(\mathbf{k}_h, \omega) / \epsilon_F,
\end{aligned} \quad (\text{B.1})$$

where we used  $G(\mathbf{k}_h + \mathbf{q} - \mathbf{Q}, \omega + \nu) \approx 1/\epsilon_F$  since  $\mathbf{k}_h + \mathbf{q} - \mathbf{Q}$  is necessarily off-shell if  $\mathbf{k}_h, \mathbf{k}_h + \mathbf{Q}$  are onshell (remember we consider incommensurate order). the vertex function  $\Lambda_{Q,h}^{(1a)}$  is not singular and may be discarded.

### Appendix B.2. Single energy fluctuation diagram

The vertex function involving a single energy fluctuation (as in Fig. 2 with  $\Gamma$  replaced by  $\chi_E$ ) is given by

$$\Lambda_Q^{(b)}(k; Q) = \Lambda_Q^4 \Lambda_v^2 \int (dq) G(k + Q + q) G(k + q) \chi_E(q) \quad (\text{B.2})$$

where  $k = (\mathbf{k}, \omega)$ ,  $Q = (\mathbf{Q}, \Omega)$  and  $q = (\mathbf{q}, \nu)$ . We are interested in the limit  $\Omega = 0$ , and in momenta  $\mathbf{k}$  on the cold part of the Fermi surface. The momentum  $\mathbf{k} + \mathbf{Q}$  is then far from the Fermi surface and we may approximate  $G(k + Q + q) \approx 1/\epsilon_F$ . The remaining expression is identical to the one for the self-energy.

$$\Lambda_Q^{(b)}(k; Q) \approx \frac{1}{\epsilon_F} \Sigma(\omega) \propto \Lambda_v^2 \Lambda_Q^{2d-1} \left( \frac{|\omega|}{\epsilon_F} \right)^{d-1/2} \quad (\text{B.3})$$

Anticipating critical behavior of the self energy,  $\Sigma(\omega) \propto \omega |\omega/\epsilon_F|^{-\eta}$ ,  $\eta > 0$ , we see that  $\Lambda_Q^{(b)} \rightarrow 0$  in the limit  $\omega \rightarrow 0$ . So, again, the vertex function  $\Lambda_Q^{(b)}$  is not singular and we will drop it.

## References

- [1] J. A. Hertz, Phys. Rev. B **14**, 1165(1976).
- [2] A. J. Millis, Phys. Rev. B **48**, 7183 (1993).
- [3] H. v. Löhneysen, A. Rosch, M. Vojta, and P. Wölfle, Rev. Mod. Phys. **79**, 1015 (2007).
- [4] S. Chakravarty, B.I. Halperin, and D.R. Nelson, Phys. Rev. Lett. **60**, 1057 (1988); Phys. Rev. B **39**, 2344 (1989).
- [5] P. Wölfle and E. Abrahams, Phys. Rev. B **84**, 041101 (2011).
- [6] E. Abrahams and P. Wölfle, Proc. Natl. Aca. Sci. **109**, 3238 (2012).
- [7] E. Abrahams, J. Schmalian, and P. Wölfle, Phys. Rev. B **90**, 045105 (2014).
- [8] S. Doniach, Physica B Amsterdam **91**, 231 (1977).  
London **413**, 804 (2001) ; Phys. Rev. B **68**, 115103 (2003).
- [9] Q. Si, Phys. Status Solidi B **247**, 476–484 (2010) and references therein.
- [10] C. Pépin, Phys. Rev. Lett. **98**, 206401 (2007); Phys. Rev. B **77**, 245129 (2008).
- [11] L. De Leo, M. Civelli, and G. Kotliar, Phys. Rev. B **77**, 075107 (2008).
- [12] T. Senthil, Ann. Phys. **321**, 1669 (2006) and references therein.
- [13] S. Sachdev, Nat. Phys. **4**, 173 (2008).
- [14] P. A. Lee, Rep.Prog. Phys. **71**, 012501 (2008).
- [15] T. Park, M. J. Graf, L. Boulaevskii, J. L. Sarrao, and J. D. Thompson, Proc. Natl. Acad. Sci. U.S.A. **105**, 6825 (2008) .
- [16] H. Shishido, R. Settai, H. Harima, and Y. Onuki, J. Phys. Soc. Jpn. **74**, 1103 (2005) .
- [17] S. K. Goh, J. Paglione, M. Sutherland, E. C. T. O’Farrell, C. Bergemann, T. A. Sayles, and M. B. Maple, Phys. Rev. Lett. **101**, 056402 (2008).
- [18] M. Vojta, Phys. Rev. B **78**, 125109 (2008).
- [19] P. Gegenwart, T. Westerkamp, C. Krellner, Y. Tokiwa, S. Paschen, C. Geibel, F. Steglich, E. Abrahams, Q. Si, Science **315**, 969 (2007).
- [20] K. Kummer, S. Patil, A. Chikina, M. Güttler, M. Höppner, A. Generalov, S. Danzenbächer, S. Seiro, A. Hannaske, C. Krellner, Yu. Kucherenko, M. Shi, M. Radovic, E. Rienks, G. Zwirgagl, K. Matho, J.W. Allen, C. Laubschat, C. Geibel, and D. V. Vyalikh, Phys. Rev. X **5**, 011028 (2015).
- [21] P. Wölfle and E. Abrahams, Phys. Rev. B **92**, 155111(2015).
- [22] P. Wölfle and E. Abrahams, Phys. Rev. B **93**, 075128 (2016).
- [23] P. S. Weiss, B. N. Narozhny, J. Schmalian, and Peter Wölfle, Phys. Rev. B **93**, 045128 (2016).
- [24] Ar. Abanov and Andrey V. Chubukov Phys. Rev. Lett. **84**, 5608 (2000).
- [25] A. Abanov, A. V. Chubukov and J. Schmalian, Adv. Phys. **52**, 119 (2003).
- [26] S. A. Hartnoll, D. M. Hofman, M. A. Metlitski, and S. Sachdev, Phys. Rev. B **84**, 125115 (2011).
- [27] V.A. Novikov, M.A. Shifman, A.I. Vainshtein, and V.I. Zakharov Nucl. Phys. **B229**, 381 (1983).

- [28] C. Stock, C. Broholm, Y. Zhao, F. Demmel, H. J. Kang, K. C. Rule, and C. Petrovic, *Phys. Rev. Lett.* **109**, 167207 (2012)
- [29] A. Schröder, G. Aeppli, R. Coldea, M. Adams, O. Stockert, H.v. Löhneysen, E. Bucher, R. Ramazashvili, and P. Coleman, *Nature* **407**, 351 (2000).
- [30] O. Stockert, H. v. Löhneysen, W. Schmidt, M. Enderle, and M. Loewenhaupt, *J. Low Temp. Phys.* **161**, 55 (2010).
- [31] A. Rosch, A. Schröder, O. Stockert, and H. v. Löhneysen *Phys. Rev. Lett.* **79**, 159 (1997).
- [32] N. Oeschler, S. Hartmann, A.P. Pikul, C. Krellner, C. Geibel, and F. Steglich, *Physica B* **403**, 1254 (2008).
- [33] H. v. Löhneysen, M. Sieck, O. Stockert, and M.Waffenschmidt, *Physica B* **223-224**, 471 (1996).
- [34] J. Custers, P. Gegenwart, H. Wilhelm, K. Neumaier, Y. Tokiwa, O. Trovarelli, C. Geibel, F. Steglich, C. Pépin, and P. Coleman, *Nature* **424**, 524 (2003).
- [35] Y. Tokiwa, T. Radu, C. Geibel, F. Steglich, P. Gegenwart, *Phys. Rev. Lett.* **104**, 096401 (2009).
- [36] P. Gegenwart, J. Custers, C. Geibel, K. Neumaier, T. Tayama, K. Tenya, O. Trovarelli, and F. Steglich, *Phys. Rev. Lett.* **89**, 056402 (2002).
- [37] L. Zhu, M. Garst, A. Rosch, and Q. Si, *Phys. Rev. B* **91**, 066404 (2003).
- [38] H. v. Löhneysen, private communication.
- [39] P. Gegenwart, Q. Si, and F. Steglich, *Nature Phys.* **4**, 186 (2008).
- [40] M. Taupin, G. Knebel, T. D. Matsuda, G. Lapertot, Y. Machida, K. Izawa, J.-P. Brison, and J. Flouquet, *Phys. Rev. Lett.* **115**, 046402 (2015).
- [41] H. v. Löhneysen, C. Pfleiderer, T. Pietrus, O. Stockert, and B. Will, *Phys. Rev. B*, **63**, 134411 (2001).
- [42] S. Hartmann, N. Oeschler, C. Krellner, C. Geibel, S. Paschen, and Frank Steglich, *Phys. Rev. Lett.* **104**, 096401 (2010).
- [43] K. Ishida, K. Okamoto, Y. Kawasaki, Y. Kitaoka, O. Trovarelli, C. Geibel, and F. Steglich, *Phys. Rev. Lett.* **89**, 107202 (2002).
- [44] This was already discussed in Ref. [5], where the result was given in terms of an unknown exponent  $\beta$ , which our scaling analysis now determines as  $\beta = -1/4$ . Hence the result reported here.
- [45] S. Kambe, H. Saka, Y. Tokunaga, G. Lapertot, T. D. Matsuda, G. Knebel, J. Flouquet and R. E. Walstedt, *Nat. Phys.* **10**, 840 (2014).